NeuroImage 236 (2021) 118088

Contents lists available at ScienceDirect

NeuroImage

journal homepage: www.elsevier.com/locate/neuroimage

Temporal dynamics of neural activity in macaque frontal cortex assessed with large-scale recordings

Thomas Decramer[a,b], Elsie Premereur[a,*], Irene Caprara[a], Tom Theys[b], Peter Janssen[a]

[a] Laboratory for Neuro- and Psychophysiology, Department of Neurosciences, KU Leuven and the Leuven Brain Institute, ON2, Herestraat 49, 3000 Leuven, Belgium
[b] Research Group Experimental Neurosurgery and Neuroanatomy, KU Leuven and the Leuven Brain Institute, Belgium

ARTICLE INFO

Keywords:
Area 45b
Grasping
Multi-electrode
Non-human primate
Premotor
Reaching
saccade

ABSTRACT

The cortical network controlling the arm and hand when grasping objects consists of several areas in parietal and frontal cortex. Recently, more anterior prefrontal areas have also been implicated in object grasping, but their exact role is currently unclear. To investigate the neuronal encoding of objects during grasping in these prefrontal regions and their relation with other cortical areas of the grasping network, we performed large-scale recordings (more than 2000 responsive sites) in frontal cortex of monkeys during a saccade-reach-grasp task. When an object appeared in peripheral vision, the first burst of activity emerged in prearcuate areas (the FEF and area 45B), followed by dorsal and ventral premotor cortex, and a buildup of activity in primary motor cortex. After the saccade, prearcuate activity remained elevated while primary motor and premotor activity rose in anticipation of the upcoming arm and hand movement. Remarkably, a large number of premotor and prearcuate sites responded when the object appeared in peripheral vision and remained active when the object came into foveal vision. Thus, prearcuate and premotor areas continuously encode object information when directing gaze and grasping objects.

1. Introduction

A network of cortical areas in posterior parietal and frontal cortex controls the planning and execution of eye-, arm- and hand movements towards objects (Andersen and Buneo, 2002; Janssen and Scherberger, 2015). Recent studies have highlighted a potential role for more anterior prefrontal regions in the grasping network. Specifically, the posterior subsector of the anterior intraparietal area (AIP) – an area critical for object grasping (Gallese et al., 1994) – is connected to area 45B, whereas the anterior subsector of AIP is connected to the anterior subsector of ventral premotor cortex (area F5a, Premereur et al., 2015b). Neurons in AIP respond selectively to objects (Murata et al., 2000), three-dimensional (Srivastava et al., 2009) and two-dimensional images of objects (Romero et al., 2012) and in many cases also very small line fragments derived from object contours (Romero et al., 2014). Neurons in the part of area 45B in prefrontal cortex that is connected to pAIP also respond selectively to images of objects, and show an even stronger preference for very small line fragments measuring a mere 1–2° (Caprara et al., 2018). These results are puzzling because they suggest that neurons in area 45B may not encode grasping affordances (which would at the minimum require a representation of object parts that can be grasped), but rather positions on the object to which the gaze can be directed in anticipation of grasping. Indeed, eye-hand coordination is crucial for object grasping and manipulation. Human observers invariably fixate grasp sites on the object before contact, and obstacles that have to be avoided when the object has to be moved. Overall, the gaze identifies landmark locations and guides hand movements in space (Johansson et al., 2001), reviewed in Flanagan et al. (2006).

To clarify how eye movement -, reaching - and grasping signals evolve when objects appear in the visual field and are subsequently manipulated, it is critical to use a task that contains all three action components. In the past, researchers have mainly employed tasks that activate the neurons in the area under study in a specific task, but have rarely investigated how these neurons behave when performing another action, e.g. how primary motor neurons respond during saccades, or FEF neurons respond during grasping. Although the signals recorded in these areas can be related to more than one function (e.g. reaching and grasping in PMv and PMd, Lehmann and Scherberger, 2013), causal manipulations of neural activity consistently highlight the functional specialization of each area (Fogassi et al., 2001; Kurata and Hoffman, 1994; Wardak et al., 2006).

To investigate how neurons in prefrontal and frontal cortex respond during eye-, arm- and hand actions towards objects, we performed unbiased large-scale (> 2000 sites) electrophysiological recordings of spiking activity. We covered a large part of frontal cortex (area 45B, FEF, PMd, PMv and M1) using a multi-electrode microdrive (Gray et al., 2007), in a

* Corresponding author.
E-mail address: elsie.premereur@kuleuven.be (E. Premereur).

https://doi.org/10.1016/j.neuroimage.2021.118088
Received 22 October 2020; Received in revised form 2 March 2021; Accepted 12 April 2021
Available online 26 April 2021

task where an eye movement to an object was followed by a reach-and-grasp movement. Intriguingly, many recording sites in prefrontal and premotor cortex responded to the object appearing in peripheral vision and remained active after the saccade had brought the object in foveal vision up to the reaching and grasping movement, suggesting a role in object processing during actions with multiple effectors.

2. Methods

All experimental procedures were performed in accordance with the National Institute of Health's *Guide for the Care and Use of Laboratory Animals* and EU Directive 2010/63/EU, and were approved by the Ethical Committee on animal experiments at KU Leuven. The animals in this study were pair or group-housed with cage enrichment (toys, foraging devices) at the primate facility of the KU Leuven Medical School. They were fed daily with standard primate chow supplemented with nuts, raisins, prunes and fresh fruits.

2.1. Subjects

We implanted 2 monkeys (macaca mulatta, Monkey A. and Monkey S.) with a semi-chronic 96 channel multi-electrode microdrive (Gray Matter research, Bozeman, United States; Gray et al., 2007) over frontal cortex (left hemisphere). This microdrive has an electrode spacing of 1.5 mm and contains 96 movable electrodes in a 1.5 × 1.5 cm box, the design allows to lower each electrode individually which renders recording from many unique sites in different areas. Both animals had received an MRI-compatible head post anchored to the skull with ceramic screws (Thomas Recording), dental acrylic and cement during propofol anesthesia.

2.2. Microdrive positioning

Preoperative magnetic resonance imaging (MRI) was performed in a 3T scanner (Siemens Trio, Forchheim, Germany) while the monkeys were sedated with a mixture of ketamine (Nimatek, Eurovet; 12.5 mg/30 min) and medetomidine (Domitor, Orion; 0.25 mg/30 min).

The animals were positioned in a stereotactic frame (Kopf Model 1430 M, Tujunga, Canada) to allow precise calculation of the coordinates for the recording cylinder (Premereur et al., 2019). To obtain high quality structural scans, three T1 MPRAGE volumes were collected and averaged (144 horizontal slices; 0.6 mm^3 isotropic voxels). MPRAGE images were collected with a receive-only custom-designed surface coil, using the standard body transmitter (total scanning duration: 30 min). The preoperative scans were used to determine the exact location of the microdrive, after which the manufacturer (Gray Matter research, Bozeman, United States) built a custom-made cylinder, fitting perfectly on the skull.

In a first surgical procedure, we implanted the cylinder (without microdrive or electrodes). At our request, a plug was designed with four reference holes, which were filled with a diluted gadolinium solution (5% solution of Dotarem 0.5 mmol/mL (Guerbet, Villepinte, France), serving as a contrast agent to estimate the anteroposterior and mediolateral border of the cylinder. After verification of the position of the cylinder using anatomical MRI, a craniotomy was performed in a second surgical procedure. After recovery, a short final procedure was performed to insert the microdrive in the cylinder and attach it to the cylinder and skull with cement.

2.3. Experimental design

2.3.1. Delayed saccade-reach-grasp task

We developed a new saccade-reach-grasp task mimicking naturalistic behavior. The experimental setup (Fig. 1) consisted of an object (size: 15 cm, 28° in diameter), with three identical graspable keys (superior/inferior/lateral spaced in a triangular fashion (10 cm apart); each having a blue LED light at the center; key size 2 cm, 3.8°; object light size 0.2°). The center of the object contained a green light (size 0.2°), the dimming of which served as the go-cue for the grasping movement. The object was positioned by a robot within a reachable distance for the monkey next to an LCD screen, at two possible positions in space, a low position and high position (10 cm above the low position). The center of the object was positioned at a distance of 30 cm from the resting position, 10 cm and 20 cm above the resting position for the low and high position, respectively. The highest and lowest graspable keys across the two robot positions were 20 cm apart. In this study, we averaged neural activity across all positions, therefore the two different robot positions will not be mentioned further. An external light illuminated the object at the start of the trial, the resting position of the hand was monitored with the interruption of a laser beam. Eye movements were monitored using an infrared tracker (EyeLink 2, SR Research), sampling the position of one eye at 500 Hz).

The LCD screen was used to present a fixation point (a small square) close to the edge of the screen at the beginning of each trial (Fig. 1). The monkey sat in the dark with its hand on the resting position, and initiated the trial when fixating a small square (0.2 × 0.2°) on the screen. After 300 ms of fixation, the external light source illuminated the object while the monkey was still fixating, the object therefore appeared in peripheral vision (center of object at 28° eccentricity, the edge of the object was located at 14° eccentricity). Together with the object lamp, one of the blue object LEDs was illuminated (indicating which object key had to be grasped), together with the green light (go cue) at the center of the object. After a variable delay (300–1100 ms) the fixation point was dimmed, which served as the saccade go-cue. Then, the monkey had to make a saccade and fixate the blue illuminated key. After a second variable delay (200–1000 ms) the green light at the center of the object dimmed, serving as a grasp go-cue. After dimming of the green light, the monkey performed a reach to grasp movement towards the illuminated object light and pulled the object key. Upon pulling the object, the monkey was rewarded with juice (Fig. 2).

2.3.2. Saccade task

For the saccade task, the screen was positioned at 90 cm from the animal. After 200 ms of fixation at the central square (0.2 × 0.2°) on the screen, a single saccade target appeared in one of ten locations in the contralateral visual hemifield. The 10 targets appeared at 5 polar angles (0 deg, +45 deg, +90 deg, −45 deg, −90 deg) and two eccentricities (either 6 or 12 deg). After a variable delay, the fixation point dimmed, instructing the monkey to make a saccade to the target (visually-guided delayed saccade task).

2.4. Electrophysiological recordings

We recorded using a 96-ch digital headstage (Cereplex M, Blackrock Microsystems, UT, USA) interfaced with a 128ch neural signal processor (Cerebus, Blackrock Microsystems, UT, USA). Single- and multi-unit signals were high-pass filtered (750–5000 Hz). To detect multiunit or background activity, the spike signal was triggered and the spike detection threshold was set at 95% of the maximum amplitude of the signal as determined in the recording period immediately prior to the start of each recording session, counting each trace passing through the threshold as a spike. For single unit analysis, additional spike sorting was performed offline (Offline Sorter 4, Plexon, TX, USA).

We recorded delayed saccade-reach-grasp sessions (monkey A.: 70, monkey S.: 59) and saccade sessions (monkey A.: $N = 40$, monkey S.: $N = 60$), in the large majority of recording days during the same sessions. The recordings took place over a period of 6 months, after which the microdrive was removed. In total across all recording sites, we recorded from 2009 responsive sites (net spikerate multi-unit activity (MUA) >3 standard errors (SE) above baseline during the saccade-reach-grasp task) in monkey A. and 1287 responsive sites in monkey S. A subset of these responsive sites (1706 in monkey A., 1120 in monkey S.) was localized

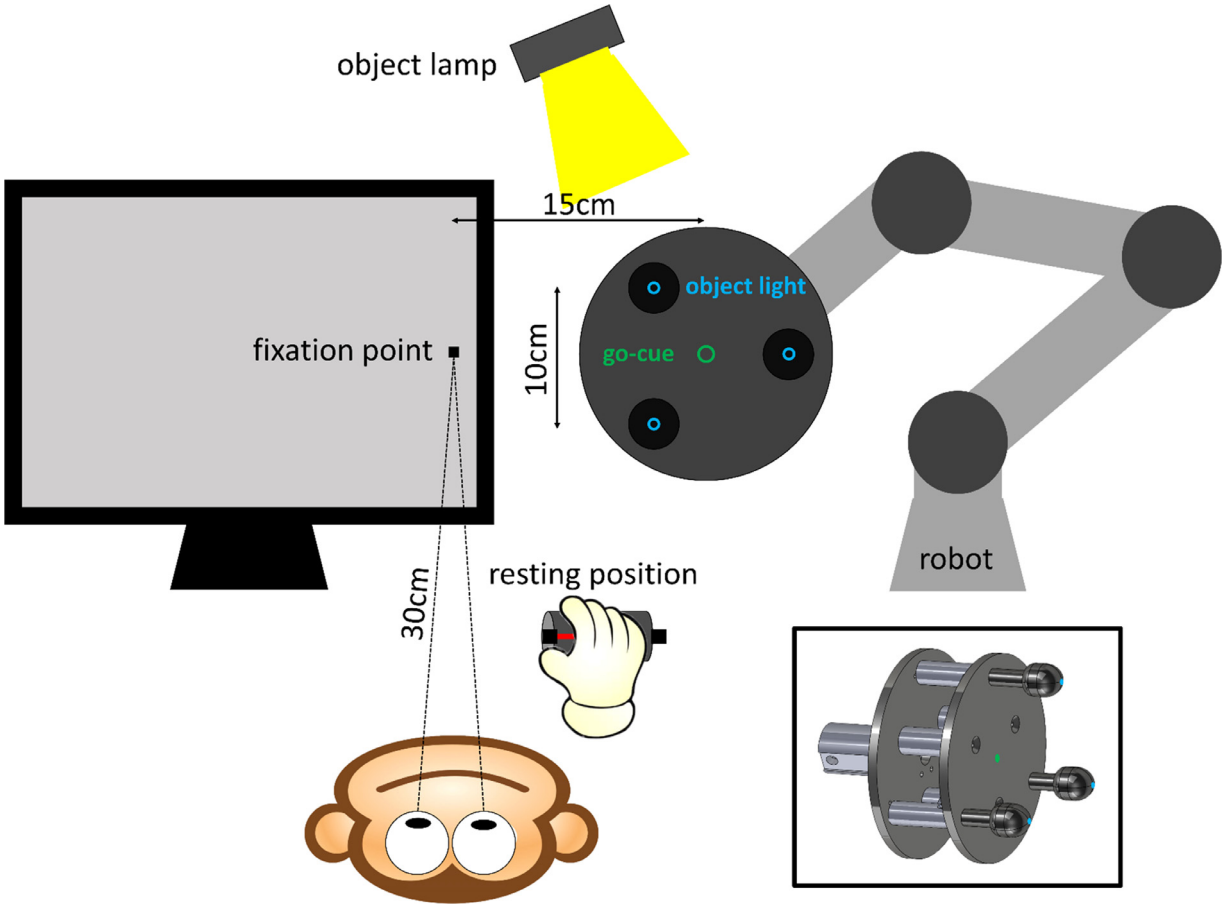

Fig. 1. *Experimental setup*. The experimental setup consisted of an object, with three identical graspable keys (see inset for 3D rendering of object) spaced in a triangular fashion, each having a blue LED light at the center. The center of the object contained a green light, the dimming of which served as a go-cue. The object was positioned by a robot within a reachable distance for the monkey next to an LCD screen. The LCD screen was used to present a fixation point (a small square) close to the edge of the screen at the beginning of each trial. An external object lamp illuminated the object at the start of the trial, the resting position of the hand was monitored with the interruption of a laser beam and eye movements were monitored using an infrared tracker.

in one of the four frontal regions we defined (see below) and included in the present study.

2.5. Electrode localization

Throughout the experiment, detailed notes were kept on which electrodes were lowered, how much they were lowered (number of turns), and the recorded activity (background activity, spiking activity or silence). Half of the electrodes were lowered at the beginning of every recording session; the other half would be lowered during the next session. Electrodes were lowered 250 μm per session (after puncturing the dura). Some electrodes were targeted to specific areas to be able to simultaneously record from all these areas.

We furthermore obtained computed tomography (CT) scans during the experiment (1x/4–6 weeks), while the monkeys were sedated with a mixture of ketamine (Nimatek, Eurovet; 12.5 mg/30 min) and medetomidine (Domitor, Orion; 0.25 mg/30 min). These high-resolution scans with artefact reduction algorithms allowed to individually visualize electrode tips (Premereur et al., 2019). During CT scanning, both monkeys were positioned in the same stereotactic frame (Kopf Model 1430 M, Tujunga, Canada) as the preoperative MRI, which allowed to easily coregister both scans in SPM12. Hybrid CT-MR images were created to anatomically reconstruct electrode trajectories using the imcalc tool in SPM12. We also verified the accuracy of our reconstruction methods by making small electrolytic lesions at the end of the recordings, which were subsequently visualized on anatomical MRI after removal of the microdrive (Premereur et al., 2019).

We categorized recording sites into four different regions, based on anatomical landmarks: pre-arcuate (preAS, anterior to the genu and inferior ramus of the arcuate sulcus), ventral premotor (PMv, posterior to arcuate sulcus and ventral to the spur of the arcuate sulcus), dorsal premotor (PMd, posterior to arcuate sulcus and dorsal to the spur) and pre-central electrodes (preCS, anterior to the central sulcus). A subset of electrodes (with double colors in Fig. 3) first travelled through the anterior bank of the arcuate sulcus (preAS) and then through the posterior bank of the arcuate sulcus (PMv). In total, we included 2826 responsive MUA sites (1706 in monkey A., 1120 in monkey S.) in the four frontal regions.

2.6. Data analysis

Data analysis was performed using custom-written Matlab (the MathWorks, MA, USA) scripts. For the MUA analysis, we subtracted the baseline activity measured during fixation of the small square on the screen (net neural response, not normalized). For every trial, the baseline response (200 ms before light onset) was subtracted from the spike rate (SR) during the entire trial. Responsive sites were defined as recording sites in which the neural activity reached more than 3 SE above the baseline activity in any trial epoch. Mean responses were calculated by averaging the net SR calculated as described above. To investigate the neural dynamics in our sequential eye-, arm- and hand movement

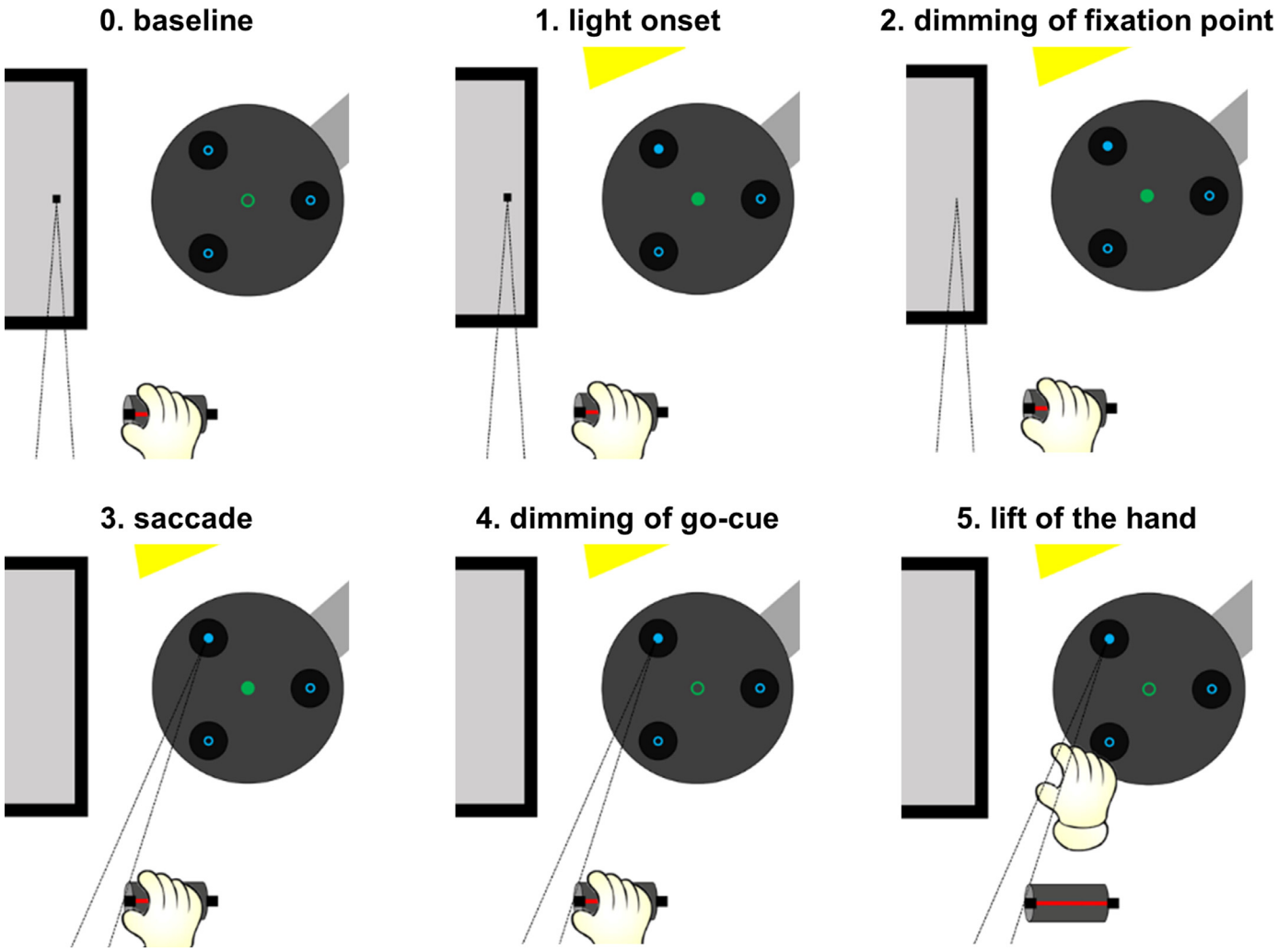

Fig. 2. *Main events in the delayed saccade-reach-grasp task*. After 300 ms of fixation ('0. baseline'), the object lamp illuminated the object ('1. light onset'). At the same time, one of the blue object lights was illuminated (indicating which object key had to be grasped), together with the green light at the center of the object. The dimming of the fixation point ('2. dimming of fixation point') served as the go-cue for the saccade ('3. saccade'). The green light at the center of the object was the go-cue for the grasping movement ('4. dimming of grasping go-cue'), after which the monkey reached ('5. lift of the hand'), grasped and pulled the object key.

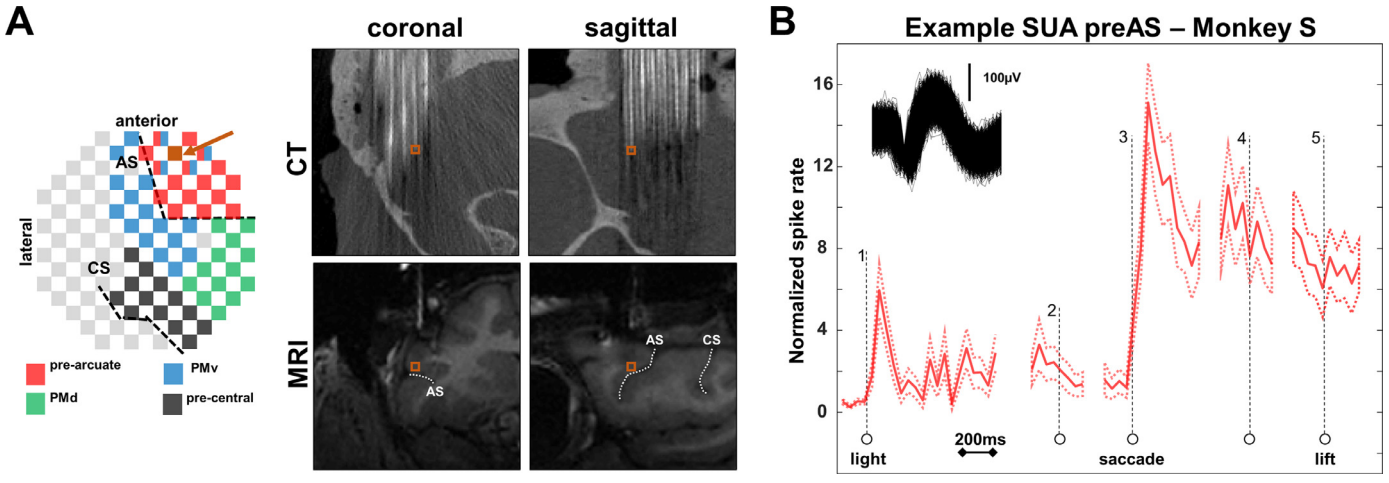

Fig. 3. *Example preAS single-unit, Monkey S*. (A) Left panel: overview of microdrive, the example electrode (orange square) is indicated with an arrow. Arcuate sulcus (AS) and central sulcus (CS) are depicted in black dotted lines in the left panel. Right panel: coronal/sagittal CT (upper) and MRI (lower) images illustrating the position of the electrode (orange square), anterior to the AS (depicted in white dotted line) in area 45B. (B) Example neuron. Mean normalized firing rate (red line) ± standard error of mean (SEM; red dotted lines) is shown, aligned to the different events in the task: light onset above the object in peripheral vision (1), saccade go-cue (2), saccade onset (3), grasp go-cue (4) and lift of the hand (5). Spike waveform is shown in inset.

task, we aligned the activity to five trial events: light onset, saccade go-cue, saccade onset, grasping go-cue and lift of the hand. Because we observed an electronic artefact in a subset of the recordings when the animal grasped the object key, we did not align the activity on the pull of the object.

To illustrate the responses of individual sites, we plotted the mean net MUA response (MUA activity minus the baseline activity measured during fixation of the small square, averaged over 200 ms before light onset) during light onset (hence object in peripheral vision) against the net neural response during object fixation (hence object in central vision). To illustrate how the neural activity evolved after light onset across the region of frontal cortex we recorded from, we mapped the MUA on the electrode layout of the microdrive, in bins of 20 ms.

The neural selectivity in the visually-guided saccade task on the preAS electrodes was illustrated by plotting the average net MUA responses to the three saccade targets evoking the highest responses and the three saccade targets evoking the lowest responses, aligned on target onset, saccade go-cue and saccade onset.

As the detection triggers were optimized for MUA, we plotted the normalized single-unit activity (SUA) for the example unit shown in Fig. 3. We calculated the normalized SUA by dividing the SR at the different trial events with the baseline before each trial (200 ms before light onset).

2.7. Statistical analysis

We analyzed the differences between the four frontal regions (preAS, PMd, PMv and preCS) in the average MUA by calculating ANOVAs on the spiking activity in different epochs of the trial (light onset, dimming of fixation point, saccade, dimming of grasping go-cue, lift of the hand) and post-hoc Tukey-Kramer tests.

To investigate the relationship between neural activity and behavior, we calculated correlation coefficients between the average MUA on all electrodes in a region and the following parameters: saccade reaction time (i.e. the time between the saccade go-cue and the saccade onset), hand reaction time (i.e. the time between the grasping go-cue and the lift of the hand), and grasping time (i.e. the time between the lift of the hand and the pull of the object). On each trial, we considered the average MUA in a 150 ms epoch before the event (saccade onset, lift of the hand). For the grasping event we avoided the artefact by averaging the MUA from 200 till 50 ms before grasp. We detrended both the behavioral measurements and the spike rates by subtracting the mean for that recording session on each trial, and calculated Pearson correlation coefficients on the detrended data. For each region, we then determined the proportion of recording sessions in which the correlation between the spike rate and the behavioral parameter was significant, and used z-tests for proportions to test for significant differences between the regions.

To determine the neuronal selectivity in the delayed saccade task, we calculated one-way ANOVA's on the MUA in three epochs of the trial (target onset, saccade go-cue and saccade onset). To assess significant differences between pre-and postsaccadic activity for the different saccade target positions, two-way ANOVAs with factors *epoch* (pre vs post) and *target position* were used.

3. Results

In total, we recorded from 2826 responsive MUA sites (1706 in monkey A., 1120 in monkey S.) in four frontal regions: the prearcuate sulcus region (preAS), which included the FEF and area 45B, PMv (consisting of areas F4 and F5), PMd (area F2) and the pre-central sulcus region (preCS), largely consisting of primary motor cortex (F1). Because we lowered approximately half of the electrodes on each recording day by 250 μm, we estimate that we obtained data in at least 1410 (850 in monkey A., 560 in monkey S.) unique recording sites.

3.1. Electrode localization and example neuron

Based on the co-registered CT and MR images, we identified the location of each electrode with respect to the arcuate sulcus (Fig. 3A, inset Fig. 4A and B). All electrodes anterior to the AS were labeled preAS ($N = 14$ in monkey A. and $N = 17$ in monkey S.). More posterior electrodes were classified as either PMv (the most lateral cluster, $N = 20$ in monkey A. and $N = 19$ in monkey S.) or PMd (the most medial cluster, $N = 20$ in monkey A. and $N = 13$ in monkey S.), whereas the most posterior electrodes located close to the central sulcus formed the preCS group ($N = 19$ and $N = 13$, respectively). A subset of electrodes ($N = 3$ in monkey A. and $N = 4$ in monkey S.) first travelled through the anterior bank of the arcuate sulcus (preAS), crossed the sulcus and finally recorded in the posterior bank of the arcuate sulcus (the F5a subsector of PMv, double-color code in Fig. 3A, inset Fig. 4A and B).

Fig. 3B illustrates a typical response of a single preAS unit in our saccade-reach-grasp task. The tip of the electrode was clearly located in the anterior bank of the AS (Fig. 3A), in area 45B (Caprara et al., 2018). Fig. 3B shows the normalized firing rate of the neuron (± standard error of mean (SEM)) (spike waveform in the inset of Fig. 3B), aligned to the different events in the task: light onset above the object in peripheral vision (1), saccade go-cue (2), saccade onset (3), grasp go-cue (4) and lift of the hand (5). This example neuron responded shortly after light onset with a transient burst of action potentials, responded very strongly after saccade onset and continued to be highly active while the animal was fixating the object, until after the lift of the hand. Thus, this preAS neuron signaled the appearance of the object in peripheral vision at an eccentricity of 30 deg in the contralateral hemifield, but remained active after the saccade had brought the object in foveal vision.

3.2. Population activity in the four frontal regions

To evaluate the differences in neural dynamics in the four frontal regions we identified, we plotted the average net MUA responses (spike rate, SR) aligned at all trial events (Fig. 4A and B). The appearance of the object in peripheral vision (*epoch 1*) triggered the fastest and strongest responses in the preAS neurons, followed by the PMd and PMv neurons (one-way ANOVA with factor area; SR calculated 0–250 ms after onset; monkey A.: $F(3) = 164.0688$, $p < 0.001$; monkey S.: $F(3) = 147.8608$, $p < 0.001$; posthoc Tukey-Kramer tests: $p < 0.001$). At this moment in the trial, we observed very little response in the preCS recording sites. After this initial visual transient, the activity in the preCS region also rose and reached the same level as preAS around the time of the saccade go-cue (*epoch 2*; SR −100–200 ms around go-cue: one-way ANOVA with factor area; monkey A.: $F(3) = 5.2056$, $p = 0.0014$; monkey S.: $F(3) = 7.61$, $p < 0.001$; posthoc Tukey-Kramer tests comparing preAS and preCS: $p > 0.70$). The next major event in the trial, saccade onset (*epoch 3*), evoked a strong burst of activity in the preAS recording sites, while the activity in the other regions continued to grow (SR 0 - 200 ms after saccade onset: one-way ANOVA with factor area; monkey A.: $F(3) = 14.3798$, $p < 0.001$; monkey S.: $F(3) = 33.8492$, $p < 0.001$; posthoc Tukey-Kramer tests comparing preAS and other areas: $p < 0.001$. As a result, the preCS activity became higher than the preAS activity just before the grasp go-cue (*epoch 4*; SR −100 - 200 ms around go-cue: one-way ANOVA with factor area; monkey A.: $F(3) = 48.0704$, $p < 0.001$; monkey S.: $F(3) = 23.9122$; $p < 0.001$; posthoc Tukey-Kramer tests comparing preAS and preCS: $p < 0.001$), although the latter spike rate was still higher than in the interval around the saccade go-cue (when the object was in peripheral vision; one-way ANOVA with factor event; monkey A.: $F(4) = 20.9965$, $p < 0.001$; monkey S.: $F(4) = 15.8356$, $p < 0.001$; posthoc Tukey-Kramer tests comparing SR for preAS around saccade- and grasp-cue: $p < 0.001$). Finally, the strongest rise in activity occurred in the pre-CS, PMd (monkey S. only) and PMv electrodes before and immediately after the lift of the hand (*epoch 5* SR 0–200 ms after lift: one-way ANOVA with factor area; monkey A.: $F(3) = 170.453$, $p < 0.001$; monkey S.: $F(3) = 28.109$, $p < 0.001$. posthoc Tukey-Kramer tests comparing

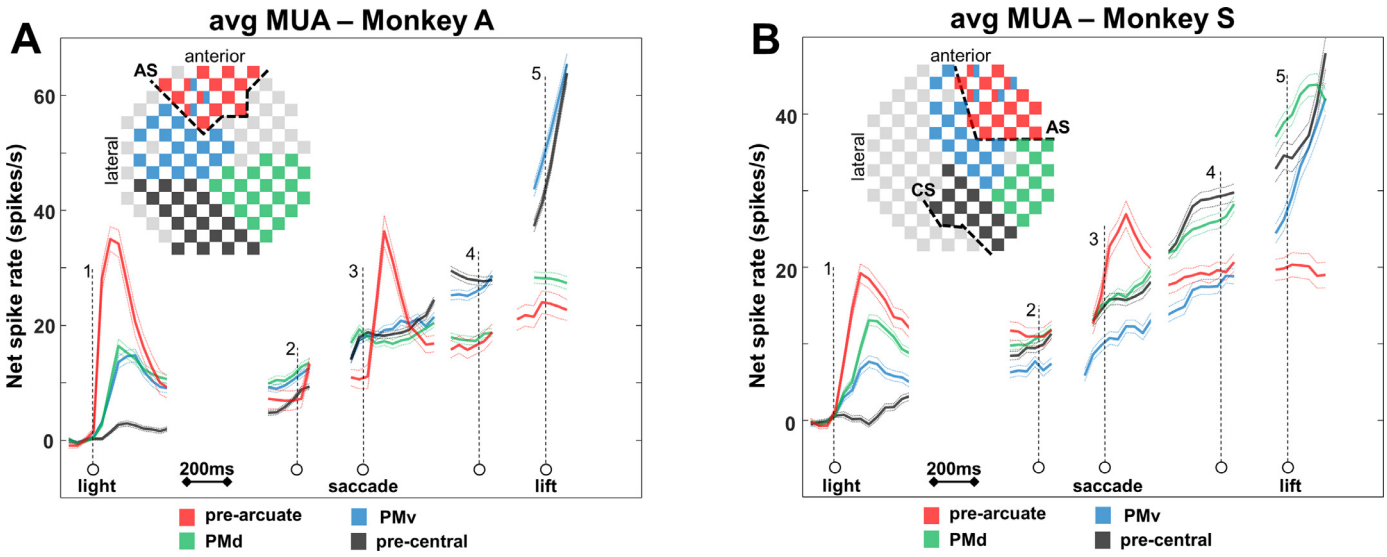

Fig. 4. *Average net MUA responses aligned at all trial events in both monkeys.* A Monkey A. Mean MUA (lines) ± SEM (dotted lines) responses aligned to the different events in the task: light onset above the object in peripheral vision (1), saccade go-cue (2), saccade onset (3), grasp go-cue (4) and lift of the hand (5). B Monkey S. With the exception of the PMd recording sites, the pattern of activity in monkey S. was highly comparable to the one observed in monkey A.

preAS and preCS/PMv/PMd (monkey S. only): p <0.001). Nonetheless, the preAS activity continued to be elevated above the level measured in the delay period before the saccade go-cue, even though no eye movement was required at this moment in the trial. With the exception of the PMd recording sites, the pattern of activity in monkey S. was highly comparable to the one observed in monkey A. Overall, the MUA responses in the four frontal regions recorded in a very large number of recording sites revealed several unexpected findings: the sustained activity in preAS neurons after the saccade was completed until after the lift of the hand, the rising activity in preCS neurons in the delay period before the saccade, and the premotor responses, which evolved together and followed a pattern between the preAS and the preCS responses.

3.3. Peripheral versus central object responses

The sustained preAS activity we observed after the animals started to fixate the to-be-grasped object may have been the result of activity emerging in another population of preAS neurons with foveal or near-foveal receptive fields (RFs). Alternatively, it is possible that the same preAS neurons responding to the appearance of the object in peripheral vision maintained a high level of activity when the object was fixated, which would imply RFs that encompassed both the central and peripheral visual field. For example, the neuron in Fig. 3 fired when the object appeared in peripheral vision, and maintained a high level of activity after the animal had made a saccade towards the object, bringing it in central vision. To decide between these two alternatives, we calculated the net MUA response in the epoch when the object was present in peripheral vision (R_{periph}) and the net MUA response when the object was fixated (hence after the saccade was completed and before the grasping go-cue was given, $R_{central}$), for every responsive MUA site. Fig. 5 shows the scatterplots in each frontal region for both animals. The red line indicates the level where $R_{central} = 2 * R_{periph}$, and the green line the level where $R_{central} = \frac{1}{2} * R_{periph}$. We then defined three types of responses: 'peripheral' MUA sites mainly responded when the object appeared in the periphery ($R_{periph} > 2 * R_{central}$), 'central' MUA sites mainly responded when the object was present in central vision ($R_{central} > 2 * R_{periph}$), and 'balanced' MUA sites responded to both central and peripheral object presentation ($\frac{1}{2} * R_{periph} < R_{central} < R_{periph} * 2$). In both monkeys, a large fraction of preAS neurons showed similar object responses in central and peripheral vision ('balanced'; 38% in monkey A. and 48% in monkey S., see Table 1). In contrast, this proportion of 'balanced' neurons was significantly lower in the preCS neurons (6% in both monkeys, z-test $p < 0.001$). PMd and PMv also contained a high proportion of balanced neurons (35 and 26% in PMd, and 30 and 25% in PMv, for monkey A. and monkey S., respectively). We also observed high proportions of balanced responses at the level of single preAS neurons, as illustrated by the example neuron in Fig. 3B (N = 208, both monkeys combined; 57% balanced; data not shown).

Table 1
Proportion of peripheral, balanced and central responsive MUA sites. In both monkeys, a large fraction of preAS neurons were balanced (38% in monkey A. and 48% in monkey S.). In contrast, this proportion of 'balanced' neurons was very low in the preCS neurons (6% in both monkeys). PMd and PMv also contained a high proportion of balanced neurons (35% and 26% in PMd, and 30 and 25% in PMv, for monkey A. and monkey S., respectively).

		Monkey A	%	Monkey S	%
pre-arcuate	Total	136	/	183	/
	Periphery	69	50.7	34	18.6
	Balanced	51	37.5	88	48.1
	Foveal	16	11.8	61	33.3
PMd	Total	309	/	347	/
	Periphery	41	13.2	8	2.3
	Balanced	109	35.3	91	26.2
	Foveal	159	51.5	248	71.5
PMv	Total	574	/	231	/
	Periphery	35	6.1	11	4.8
	Balanced	173	30.1	58	25.1
	Foveal	366	63.8	162	70.1
pre-central	Total	687	/	359	/
	Periphery	7	1.0	2	0.5
	Balanced	44	6.4	20	5.6
	Foveal	636	92.6	337	93.9

3.4. Correlation with behavior

Overal performance was highly similar between both animals: Monkey. A. performed 3657 out of 11,169 (32.7%) and Monkey S. performed 3242 out of 8367 (38.7%) trials correctly. Average saccade RT was 233 ± 2 ms (SEM) for Monkey A. and 242 ± 3 ms for Monkey S.; average lift RT was 430 ± 8 ms for Monkey A. and 412 ± 7 ms for Monkey S.;

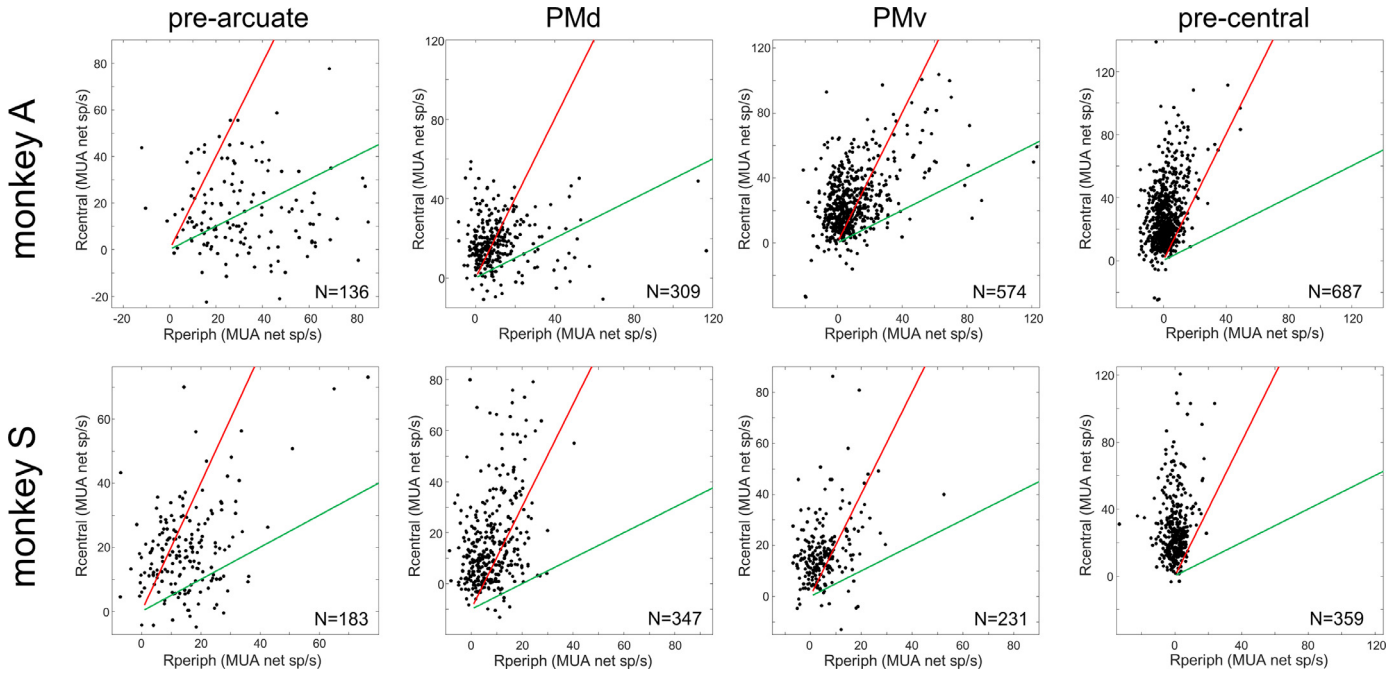

Fig. 5. *Peripheral vs central object responses across the four frontal regions.* Scatterplots depict the average net MUA response to objects in peripheral vision (Rperiph) against the MUA response to the objects in central position (Rcentral), in each frontal region for both animals. The number of recordings sites in these regions is shown in the lower right corner of each graph. The red line indicates the level where $R_{central} = 2 * R_{periph}$, and the green line the level where $R_{central} = \frac{1}{2} * R_{periph}$. 'Peripheral' MUA sites mainly responded when the object appeared in the periphery ($R_{periph} > 2 * R_{central}$), 'central' MUA sites mainly responded when the object was present in central vision ($R_{central} > 2 * R_{periph}$), and 'balanced' MUA sites responded to both central and peripheral object presentation ($\frac{1}{2} * R_{periph} < R_{central} < R_{periph} * 2$).

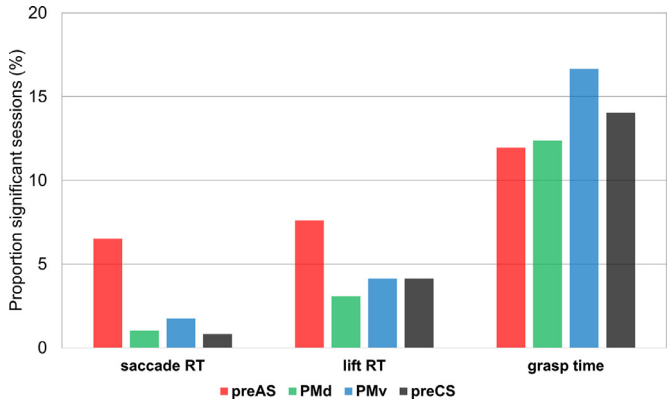

Fig. 6. *Proportion of recording sessions with significant correlations between neural response and behavior.* The proportion of significant sessions (%) are indicated for the four frontal areas (preAS, PMd, PMv and preCS) and for the three different behavioral measures (saccade reaction time, lift of the hand reaction time and grasp time).

and average grasp time was 377 ± 8 ms for Monkey A. and 445 ± 5 ms for Monkey S.

To determine for each frontal region the extent to which the neural activity correlated with behavior in different epochs of the trial, we calculated Pearson correlation coefficients between the detrended neural responses and the saccade RT, the lift RT and the grasping time (see Methods). In the first trial epoch (saccade onset), the preAS recording sites were significantly more likely to show negative correlations with the saccade RT than the other frontal regions, which showed very low proportions of significant correlations (Fig. 6 and Table 2 for *p*-values and *z*-scores). In the next trial epoch (lift of the hand), the activity on the preAS electrodes was still more frequently negatively correlated with the Lift RT than the activity on the PMv electrodes ($p = 0.02$). In the last trial epoch (pull of the object), the proportion of sessions with significant negative correlations between neural activity and grasping time rose markedly for every frontal region (between 10 and 17.5% of the sessions with significant correlations). Importantly, the proportion of significant correlations did not differ between the preAS and the other frontal regions (Table 2). These results indicate that the preAS activity was associated with the grasping time similar to the other frontal regions we recorded from, suggesting a similar involvement in the grasping movement.

3.5. Temporal dynamics

To illustrate the temporal dynamics of the neural response across all electrodes in the four frontal regions, we mapped the activity onto the outline of the microelectrode array, in 20 ms bins (Fig. 7 (monkey A.), Fig. S1 (monkey S.)). In the first 60 ms after light onset, the activity emerged exclusively in the preAS region, spreading to the PMd and PMv electrodes around 80–100 ms after light onset. However, although the average population response in this epoch of the trial was still very low (Fig. 4), individual preCS recording sites also became active as early as 100–120 ms after light onset (see arrow in Fig. 5 at the 120 ms bin).

3.6. Comparison with standard delayed saccade task

Finally, to allow a direct comparison between our saccade subtask (in which the target object remained present) and a standard delayed-saccade task with targets on a display (which disappear after the saccade), we recorded the MUA on the preAS electrodes ($N = 241$ in monkey A. and $N = 452$ in monkey S.) while the animals performed visually-guided saccades to 10 targets in the contralateral hemifield. Fig. 8 shows the average MUA response of all recording sites with a significant visual response (> 3 SE above baseline) to the three targets eliciting the strongest and the weakest response, aligned on target onset, saccade

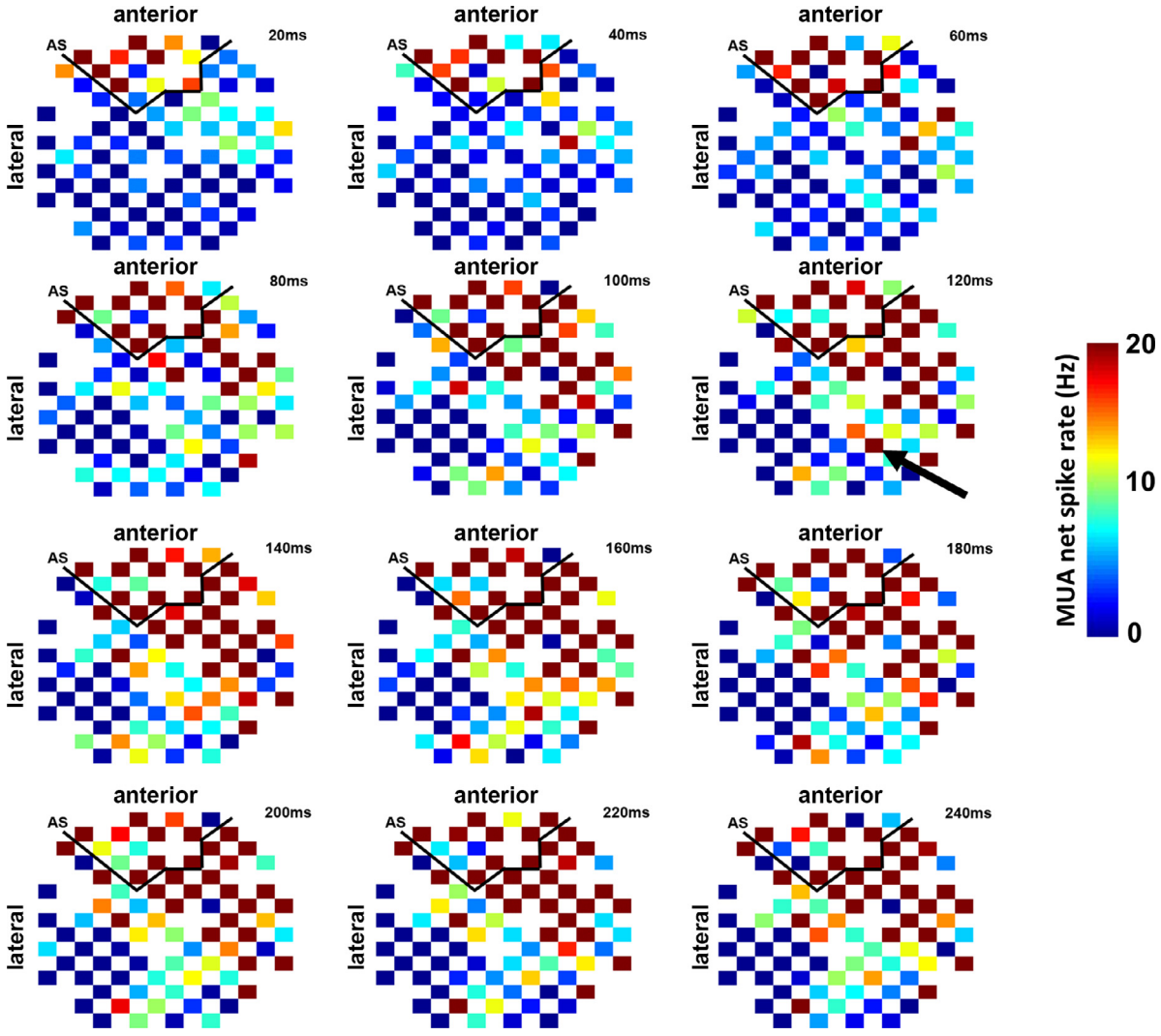

Fig. 7. *Temporal dynamics of MUA responses (Hz) across all electrodes for monkey A. after light-onset.* In the first 60 ms after light onset, the activity emerged exclusively in the preAS region, spreading to the PMd and PMv electrodes around 80–100 ms after light onset. The arrow at 120 ms depicts a preCS recordings site which activates early after light onset. For the temporal dynamics of Monkey S., see Fig. S1.

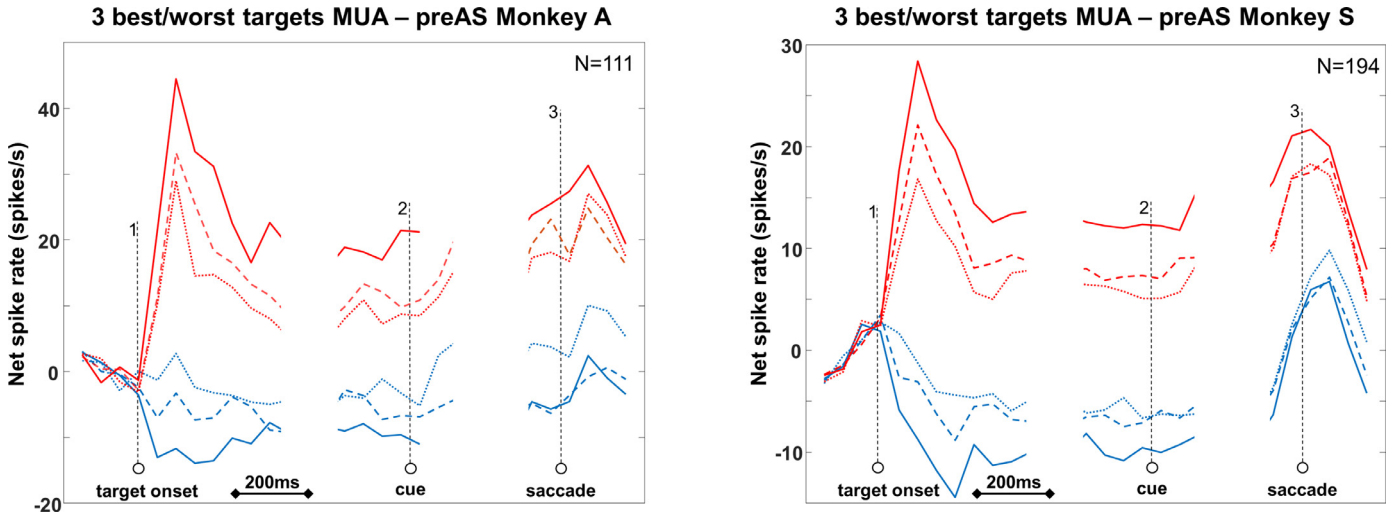

Fig. 8. *Delayed-saccade task*. Average MUA response of all preAS recordings sites (Monkey A. $N = 111$, Monkey S. $N = 194$) with significant visual response for the three best targets (depicted in red), and three worst targets (depicted in blue).

Table 2
*Number of recording sessions with significant correlation between neural activity and saccade RT, Lift RT and Grasping time for the four frontal regions across both monkeys. P- and Z-values (values indicated with * $p < 0.05$) indicate the results of the comparison with the preAS region (z-test for proportions).*

	preCS	PMd	PMv	preAS
Saccade RT	1/121 (0.8%)	1/97 (1.0%)	2/114 (1.7%)	6/92 (7.6%)
	$p = 0.005^*$	$p = 0.012^*$	$p = 0.02^*$	
	$Z=-2.6^*$	$Z=-2.25^*$	$Z=-2.04^*$	
Lift RT	5/121 (4%)	3/97 (3.1%)	2/114 (1.75%)	7/92 (7.6%)
	$p = 0.14$	$p = 0.08$	$p = 0.02^*$	
	$Z=-1.09$	$Z=-1.39$	$Z=-2.07^*$	
Grasp time	17/121 (14.0%)	12/97 (12.4%)	19/114 (16.7%)	11/92 (11.9%)
	$p = 0.33$	$p = 0.46$	$p = 0.17$	
	$Z=-0.45$	$Z=-0.09$	$Z=-0.95$	

go-cue and saccade onset. In both monkeys, preAS neurons responded fast and selectively to target onset at the preferred position (one-way ANOVA with factor target position: monkey A.: $F(9)=90.14$, $p < 0.001$; monkey S.:$F(9) = 93.73$, $p < 0.001$), showed sustained selective activity in the delay period preceding the saccade go-cue (one-way ANOVA with factor target position: monkey A.: $F(9)=30.53$, $p < 0.001$; monkey S.: $F(9) = 29.96$, $p < 0.001$), a strong perisaccadic burst of activity for all target positions (average activity post- vs pre-saccade onset, two-way ANOVA with factors pre- vs postsaccadic activity and target position: main effect of pre-vs post saccadic: $F(1) = 11.63$; $p = 0.0007$ and $F(1) = 168.24$), $p < 0.001$ for monkey A. and S., respectively; interaction between pre- and postsaccadic activity and target position, $F = 0.38$, $p = 0.95$ and $F = 1.89$, $p = 0.05$ for monkey A. and S., respectively) and a drop in response after saccade execution. Overall, this response pattern is highly similar to previous observations in the FEF using a delayed visually-guided saccade task, but did not contain the marked postsaccadic burst of activity we measured in our saccade-reach-grasp task. This difference in activity after the saccade suggests that the continued presence of the object after the saccade was critical for the postsaccadic response we observed in the saccade-reach-grasp task. Note however that the stimuli in the delayed saccade task appeared on a display beyond peripersonal space (90 cm), which may have affected the neuronal responses.

4. Discussion

We recorded the activity in a large number of sites in multiple frontal areas during a saccade-reach-grasp task, in which the target of the saccadic eye movement became the to-be-grasped object after saccade execution.

The analysis of the average spiking activity revealed a number of interesting observations. The onset of light above the object in peripheral vision first activated the preAS neurons, followed by PMd and PMv neurons, whereas preCS neurons responded weakly. Subsequently, we measured a strong post-saccadic burst of activity in preAS neurons and a steep rise in activity in PMv and preCS neurons around the lift of the hand, in line with previous studies. However, more unexpectedly we observed that preAS activity remained elevated even though the saccade had been executed and the object was now in foveal vision, and that preCS activity already rose in the delay period before the saccade, although the reach- and grasp movement occurred much later. The latter two findings indicate that the entire frontal network is engaged in all task epochs when different effectors are activated sequentially. At the level of individual recording sites, we showed that a substantial proportion of the neurons – mainly preAS but also PMd and PMv – responded strongly to the same object in peripheral vision and in central vision. Thus, large-scale simultaneous recordings reveal the neural dynamics in frontal areas when an object appears in peripheral vision and subjects plan and execute actions with different effectors.

We implemented combined CT-MR imaging to reconstruct the anatomical locations of each electrode during the experiment (Premereur et al., 2019). Therefore, although the exact boundaries between cortical areas can be difficult to determine, we are confident that the overall classification of the recording sites was accurate.

Our main finding is that many recording sites in area 45B, FEF, and to a lesser degree in PMd and PMv responded to the object appearing in peripheral vision and remained active when the saccade had brought the object into foveal vision. Activity in such clusters of neurons can track the object independent of its position in the visual field and despite the intervening saccade, while motor activity is building up in preparation of the reach and grasp movement. The fast responses observed in the preAS sites also clarify the functional significance of the flow of visual information from 3D-shape selective sites in pAIP to area 45B (Premereur et al., 2015b). Indeed, relatively early in the processing pathway and in parallel with the well-known aAIP – F5a – F5p – M1 pathway, visual information about object shape and/or location reaches prefrontal cortex, which could be useful to program saccades and hand movements even before the object is foveated. It should be noted that we measured preAS responses at very short latencies (60 ms), consistent with a previous study showing that 45B neurons respond to images of objects at very short latencies (50–60 ms (Caprara et al., 2018)). These fast responses indicate that some object information reaches the prearcuate cortex even before neurons in inferotemporal cortex respond, which may underly the rapid detection of objects, faces and animals in natural scenes observed in humans and monkeys (Mace et al., 2005; Wu et al., 2015).

The analysis of the correlations between neural activity and behavior in each of the frontal regions confirmed the hypothesis that preAS activity is involved in every epoch of the task. The higher proportion of significant correlations with the saccade RT was expected for the preAS region, but more surprising was our finding that preAS activity correlated with the grasping time to the same degree as the other frontal regions. This result strongly suggests that preAS activity is also important in the reach and grasp phase of the task. For the interpretation of our results, it is also important to note that reversible inactivation of area 45B using muscimol induces a deficit in visually-guided object grasping, similar in size to the effect of reversible inactivation of PMv ((Caprara and Janssen, 2019), Soc Neurosci abstract 2019). Hence, the elevated preAS activity we measured here after the saccade is likely causally related to object grasping, and therefore most likely highly relevant for eye-hand coordination. Specifically, neurons signaling the appearance of an object that will have to be grasped can first be involved in planning the appropriate saccade towards the object, and then remain active to guide the hand towards the appropriate grasp location on the object. Consistent with this idea are the observations by Caprara et al. (2018) that 45B (and FEF) neurons responsive to images of objects respond even stronger to very small fragments of the object contour, which may represent saccade or grasp locations on the object.

The preAS responses in the saccade-reach-grasp task differed markedly from those obtained in the standard delayed saccade task mainly by the absence of a strong postsaccadic burst of activity when the animals made saccades to targets on a display. Undoubtedly, the continued presence of the object that would become the target of the ensuing reach and grasp movement was critical in this respect. The importance

of the object in foveal vision is also demonstrated by the persistently elevated activity in preAS recording sites until after the object was grasped, indicating that these cortical sites were continuously encoding the object despite large shifts in the retinal location of that object.

In this study, we averaged the activity across the three different reach directions, and we did not test different grip types (the three object keys to be grasped were identical). Neural selectivity for reach direction and grip type is well documented in PMd (Hendrix et al., 2009; Raos et al., 2004) and PMv (Bonini et al., 2012; Fluet et al., 2010; Murata et al., 2000), and was not the focus of our study. Moreover, searching for the optimal reach direction and/or grip type is virtually impossible when recording with a large number of electrodes.

In contrast to previous studies, we report data obtained in a very large number of recording sites over a large part of frontal cortex, from M1 posteriorly to area 45B anteriorly. Because the electrodes we used were long and movable, we were able to reach cortical sites buried in sulci (such as the anterior and posterior bank of the inferior ramus of the arcuate sulcus), and record in more than 2000 unique recording sites. Since we recorded every 250 μm along the track of an electrode, the data we present here are an unbiased estimate of the actual neural responses in each of the frontal regions. We only analyzed responsive recording sites (showing activity > 3 SE above the baseline in any epoch of the trial), but averaging all recording sites (responsive and unresponsive), or changing the response criterion (2 SE instead of 3 SE) did not change the main results. A major advantage of our approach is that we could record spiking activity over a large part of frontal cortex (15 by 15 mm), including cortex buried in sulci, at very high temporal resolution. Functional imaging techniques would not be able to provide such detailed information since they either suffer from low temporal resolution (in the case of fMRI (Premereur et al., 2015a)), or can only measure at the cortical surface, as is the case for intrinsic optical imaging (Lu et al., 2017) or 2 photon imaging (Li et al., 2017).

Because the arcuate sulcus was the most important landmark in our recording area, we grouped our recording sites into four main categories: preAS, PMd, PMv and preCS. The latter recording category included primary motor cortex (area M1 or F1), but also the most caudal part of PMv (area F4). Previous studies have demonstrated that the boundary between F1 and F4 is difficult to determine, since the neural properties and the electrical excitability of the two areas are highly similar (Maranesi et al., 2012). The preAS recording sites encompassed both the FEF and the more anteriorly located area 45B. In a previous study (Caprara et al., 2018), we demonstrated that the FEF and 45B differ mainly in the location of their RF (eccentric in the FEF and parafoveal in 45B), but that both areas are similar when tested with images of objects.

Can attention partially explain why preAS neurons remained active after saccade execution? The neural effects of attention are mostly evident when different objects or locations are potentially relevant for behavior (Desimone and Duncan, 1995), but in our experimental task, there was only one object to be grasped in every trial. Therefore, competition between different objects in our task was absent. Moreover, in the delay period before the go-cue for the hand movement and after the saccade, the object was fixated and no distractors were present. Therefore, we believe it is highly unlikely that attention can explain our observations. Note that Bichot et al. (2015) demonstrated a causal role of a prefrontal site anterior to the arcuate sulcus (termed ventral prearcuate region or VPA) in feature-based attention. However, because our preAS recording sites were almost all located in the anterior bank of the arcuate sulcus, there was no significant overlap with this VPA region. Undoubtedly, the delay periods in our task (before the saccade go-cue and before the grasping go-cue) may have allowed the activation of high-level cognitive control signals, which might explain some of the elevated preAS activity after the saccade. Future experiments should investigate the exact nature of this elevated preAS activity. Importantly, the neural activity in the preAS region correlated as much with the grasping time as the activity in the other frontal regions, suggesting that preAS activity is also relevant for the execution of the object grasping action under visual guidance.

Our results provide a new view on the neural dynamics in frontal cortex when objects appear in peripheral vision and are subsequently grasped. Our approach with 96 movable electrodes furnishes more data on an order of magnitude more unique recording sites compared to recordings with a single electrode or even with multielectrode arrays. As such, the combination of high spatiotemporal resolution and a large coverage across multiple cortical areas (including access to areas buried in sulci) represents a crucial addition to the repertoire of research techniques filling the space between standard single- and multielectrode recordings and functional imaging in monkeys.

Declaration of Competing Interest

We have no conflict of interest.

Credit authorship contribution statement

Thomas Decramer: Formal analysis, Investigation, Writing – original draft, Writing – review & editing, Visualization. **Elsie Premereur:** Conceptualization, Methodology, Software, Formal analysis, Writing – original draft, Writing – review & editing, Visualization. **Irene Caprara:** Investigation. **Tom Theys:** Conceptualization, Writing – original draft, Writing – review & editing, Supervision, Funding acquisition. **Peter Janssen:** Conceptualization, Methodology, Writing – original draft, Writing – review & editing, Visualization, Supervision, Funding acquisition.

Acknowledgments

We thank Stijn Verstraeten, Piet Kayenbergh, Gerrit Meulemans, Marc De Paep, Wouter Depuydt, Walter Coudyzer, Inez Puttemans, Christophe Ulens for technical assistance. We thank Astrid Hermans and Sara De Pril for administrative support.

This work was supported by Fonds Wetenschappelijk onderzoek (FWO) Odysseus grant G.0007.12 and KU Leuven grant C14/18/100.

Tom Theys is supported by FWO (senior clinical researcher, FWO 1830717N) and Elsie Premereur received an FWO grant (FWO 1516015N).

Supplementary materials

Supplementary material associated with this article can be found, in the online version, at doi:10.1016/j.neuroimage.2021.118088.

References

Andersen, R.A., Buneo, C.A., 2002. Intentional maps in posterior parietal cortex. Annu. Rev. Neurosci. 25, 189–220. doi:10.1146/annurev.neuro.25.112701.142922.

Bichot, N.P., Heard, M.T., DeGennaro, E.M., Desimone, R., 2015. A source for feature-based attention in the prefrontal cortex. Neuron 88 (4), 832–844. doi:10.1016/j.neuron.2015.10.001.

Bonini, L., Ugolotti Serventi, F., Bruni, S., Maranesi, M., Bimbi, M., Simone, L., Fogassi, L., 2012. Selectivity for grip type and action goal in macaque inferior parietal and ventral premotor grasping neurons. J. Neurophysiol. 108 (6), 1607–1619. doi:10.1152/jn.01158.2011.

Caprara, I., Janssen, P., 2019. The causal role of three frontal areas in object grasping. Paper presented at the Society for Neuroscience 2019.

Caprara, I., Premereur, E., Romero, M.C., Faria, P., Janssen, P., 2018. Shape responses in a macaque frontal area connected to posterior parietal cortex. Neuroimage 179, 298–312. doi:10.1016/j.neuroimage.2018.06.052.

Desimone, R., Duncan, J., 1995. Neural mechanisms of selective visual attention. Annu. Rev. Neurosci. 18, 193–222. doi:10.1146/annurev.ne.18.030195.001205.

Flanagan, J.R., Bowman, M.C., Johansson, R.S., 2006. Control strategies in object manipulation tasks. Curr. Opin. Neurobiol. 16 (6), 650–659. doi:10.1016/j.conb.2006.10.005.

Fluet, M.C., Baumann, M.A., Scherberger, H., 2010. Context-specific grasp movement representation in macaque ventral premotor cortex. J. Neurosci. 30 (45), 15175–15184. doi:10.1523/JNEUROSCI.3343-10.2010.

Fogassi, L., Gallese, V., Buccino, G., Craighero, L., Fadiga, L., Rizzolatti, G., 2001. Cortical mechanism for the visual guidance of hand grasping movements in the monkey: a reversible inactivation study. Brain 124 (Pt 3), 571–586. doi:10.1093/brain/124.3.571.

Gallese, V., Murata, A., Kaseda, M., Niki, N., Sakata, H., 1994. Deficit of hand preshaping after muscimol injection in monkey parietal cortex. Neuroreport 5 (12), 1525–1529. doi:10.1097/00001756-199407000-00029.

Gray, C.M., Goodell, B., Lear, A., 2007. Multichannel micromanipulator and chamber system for recording multineuronal activity in alert, non-human primates. J. Neurophysiol. 98 (1), 527–536. doi:10.1152/jn.00259.2007.

Hendrix, C.M., Mason, C.R., Ebner, T.J., 2009. Signaling of grasp dimension and grasp force in dorsal premotor cortex and primary motor cortex neurons during reach to grasp in the monkey. J. Neurophysiol. 102 (1), 132–145. doi:10.1152/jn.00016.2009.

Janssen, P., Scherberger, H., 2015. Visual guidance in control of grasping. Annu. Rev. Neurosci. 38, 69–86. doi:10.1146/annurev-neuro-071714-034028.

Johansson, R.S., Westling, G., Backstrom, A., Flanagan, J.R., 2001. Eye-hand coordination in object manipulation. J. Neurosci. 21 (17), 6917–6932.

Kurata, K., Hoffman, D.S., 1994. Differential effects of muscimol microinjection into dorsal and ventral aspects of the premotor cortex of monkeys. J. Neurophysiol. 71 (3), 1151–1164. doi:10.1152/jn.1994.71.3.1151.

Lehmann, S.J., Scherberger, H., 2013. Reach and gaze representations in macaque parietal and premotor grasp areas. J. Neurosci. 33 (16), 7038–7049. doi:10.1523/JNEUROSCI.5568-12.2013.

Li, M., Liu, F., Jiang, H., Lee, T.S., Tang, S., 2017. Long-term two-photon imaging in awake macaque monkey. Neuron 93 (5), 1049–1057. doi:10.1016/j.neuron.2017.01.027, e1043.

Lu, H.D., Chen, G., Cai, J., Roe, A.W., 2017. Intrinsic signal optical imaging of visual brain activity: tracking of fast cortical dynamics. Neuroimage 148, 160–168. doi:10.1016/j.neuroimage.2017.01.006.

Mace, M.J., Richard, G., Delorme, A., Fabre-Thorpe, M., 2005. Rapid categorization of natural scenes in monkeys: target predictability and processing speed. Neuroreport 16 (4), 349–354. doi:10.1097/00001756-200503150-00009.

Maranesi, M., Roda, F., Bonini, L., Rozzi, S., Ferrari, P.F., Fogassi, L., Coude, G., 2012. Anatomo-functional organization of the ventral primary motor and premotor cortex in the macaque monkey. Eur. J. Neurosci. 36 (10), 3376–3387. doi:10.1111/j.1460-9568.2012.08252.x.

Murata, A., Gallese, V., Luppino, G., Kaseda, M., Sakata, H., 2000. Selectivity for the shape, size, and orientation of objects for grasping in neurons of monkey parietal area AIP. J. Neurophysiol. 83 (5), 2580–2601. doi:10.1152/jn.2000.83.5.2580.

Premereur, E., Decramer, T., Coudyzer, W., Theys, T., Janssen, P., 2019. Localization of movable electrodes in a multi-electrode microdrive in nonhuman primates. J. Neurosci. Methods, 108505 doi:10.1016/j.jneumeth.2019.108505.

Premereur, E., Janssen, P., Vanduffel, W., 2015a. Effector specificity in macaque frontal and parietal cortex. J. Neurosci. 35 (8), 3446–3459. doi:10.1523/JNEUROSCI.3710-14.2015.

Premereur, E., Van Dromme, I.C., Romero, M.C., Vanduffel, W., Janssen, P., 2015b. Effective connectivity of depth-structure-selective patches in the lateral bank of the macaque intraparietal sulcus. PLOS Biol. 13 (2), e1002072. doi:10.1371/journal.pbio.1002072.

Raos, V., Umilta, M.A., Gallese, V., Fogassi, L., 2004. Functional properties of grasping-related neurons in the dorsal premotor area F2 of the macaque monkey. J. Neurophysiol. 92 (4), 1990–2002. doi:10.1152/jn.00154.2004.

Romero, M.C., Pani, P., Janssen, P., 2014. Coding of shape features in the macaque anterior intraparietal area. J. Neurosci. 34 (11), 4006–4021. doi:10.1523/JNEUROSCI.4095-13.2014.

Romero, M.C., Van Dromme, I., Janssen, P., 2012. Responses to two-dimensional shapes in the macaque anterior intraparietal area. Eur. J. Neurosci. 36 (3), 2324–2334. doi:10.1111/j.1460-9568.2012.08135.x.

Srivastava, S., Orban, G.A., De Maziere, P.A., Janssen, P., 2009. A distinct representation of three-dimensional shape in macaque anterior intraparietal area: fast, metric, and coarse. J. Neurosci. 29 (34), 10613–10626. doi:10.1523/JNEUROSCI.6016-08.2009.

Wardak, C., Ibos, G., Duhamel, J.R., Olivier, E., 2006. Contribution of the monkey frontal eye field to covert visual attention. J. Neurosci. 26 (16), 4228–4235. doi:10.1523/JNEUROSCI.3336-05.2006.

Wu, C.T., Crouzet, S.M., Thorpe, S.J., Fabre-Thorpe, M., 2015. At 120 msec you can spot the animal but you don't yet know it's a dog. J. Cognit. Neurosci. 27 (1), 141–149. doi:10.1162/jocn_a_00701.